fzr-1 and *lin-35*/Rb function redundantly to control cell proliferation in *C. elegans* as revealed by a nonbiased synthetic screen

David S. Fay,[1,2] Sean Keenan, and Min Han[2]

Howard Hughes Medical Institute and Department of Molecular, Cellular, and Developmental Biology, University of Colorado, Boulder, Colorado 80309-0347, USA

We report here a synthetic-lethal screen in *Caenorhabditis elegans* that overcomes a number of obstacles associated with the analysis of functionally redundant genes. Using this approach, we have identified mutations that synthetically interact with *lin-35*/Rb, a SynMuv gene and the sole member of the Rb/pocket protein family in *C. elegans*. Unlike the original SynMuv screens, our approach is completely nonbiased and can theoretically be applied to any situation in which a mutation fails to produce a detectable phenotype. From this screen we have identified *fzr-1*, a gene that synthetically interacts with *lin-35* to produce global defects in cell proliferation control. *fzr-1* encodes the *C. elegans* homolog of Cdh1/Hct1/FZR, a gene product shown in other systems to regulate the APC cyclosome. We have also uncovered genetic interactions between *fzr-1* and a subset of class B SynMuv genes, and between *lin-35* and the putative SCF regulator *lin-23*. We propose that *lin-35*, *fzr-1*, and *lin-23* function redundantly to control cell cycle progression through the regulation of cyclin levels.

Genetic redundancy is a common feature of all eukaryotes, ensuring both a high degree of regulatory control and protection against mutational assault. It is also an impediment to biologists seeking to determine gene function through forward and reverse genetic approaches. Mutations in functionally redundant genes may show no obvious phenotype on their own but, when present in specific combinations, can lead to severe defects (i.e., a synthetic phenotype). Therefore, the ability to assign functions to this class of genes based solely on the availability and analysis of single mutants may be difficult or impossible.

Estimates from yeast suggest that ~40% of all genes may fail to show even weak phenotypes when deleted (Smith et al. 1996; Winzeler et al. 1999), whereas a recent large-scale functional analysis of *Caenorhabditis elegans* genes using RNAi methods failed to detect phenotypes for >85% of the genes examined (Fraser et al. 2000). In addition, recent small-scale deletion studies as well as previous mutational analyses suggest that functional disruptions of most genes in *C. elegans* fail to produce

obvious phenotypic effects (for review, see Hodgkin 2001). This apparent lack of an observable gene function may be the result of limitations at the level of detection as well as in the methodology used in the case of RNAi analysis. However, it is also likely a consequence of functional overlap conferred by either structurally related proteins or by molecularly distinct but functionally connected pathways. Evidence from yeast suggests that this latter explanation may, in fact, be the more common cause of genetic redundancy (Winzeler et al. 1999; for review, see Tautz 2000; Wagner 2000).

Given the difficulties in detecting synthetic interactions, relatively few examples of such nonhomologous genetic redundancies have been well characterized in *C. elegans* (Culotti et al. 1981; Johnson et al. 1981; Ferguson and Horvitz 1989; Davies et al. 1999). The best-known case of functional redundancy in *C. elegans* is the synthetic multivulval (SynMuv) genes (Ferguson et al. 1987; Ferguson and Horvitz 1989; for review, see Fay and Han 2000). SynMuv genes act in opposition to Ras/Map kinase pathway signaling to prevent the adoption of ectopic vulval cell fates during postembryonic development (Ferguson et al. 1987; Lu and Horvitz 1998). The relatively straightforward identification of SynMuv genes was made feasible by the ease with which Muv animals can be detected, the normally rare incidence of Muv animals in mutagenized populations, and the fact that double mutants are generally viable. SynMuv genes are

commonly assigned membership into one of two classes, A or B. Pairwise combinations of mutations in both a class A gene and a class B gene lead to the expression of the Muv phenotype (Ferguson and Horvitz 1989).

The past several years have seen the molecular identification of many SynMuv genes through both forward and reverse genetic approaches. Although some encode peptides with unknown cellular or biochemical functions, a sizable fraction of class B genes have been linked (based on sequence homology) to transcriptional repression mechanisms. These include multiple members of the NuRD (nucleosome remodeling and histone deacetylase) complex (Lu and Horvitz 1998; Solari and Ahringer 2000; von Zelewsky et al. 2000), E2F and its binding partner Dp (Ceol and Horvitz 2001), and the solitary *C. elegans* Rb/pocket protein homolog LIN-35 (Lu and Horvitz 1998).

In dramatic contrast to Rb knockout mutations in flies and mice (Clarke et al. 1992; Jacks et al. 1992; Lee et al. 1992; Du and Dyson 1999; for review, see Lipinski and Jacks 1999), strong loss-of-function (LOF) mutations in *lin-35* are not lethal and have relatively subtle effects on viability and development (Lu and Horvitz 1998; this paper). Thus, based on the SynMuv screens, the single function ascribed to *lin-35* affected only a small number of postembryonic blast cells and, moreover, required the presence of a second-site mutation to be revealed. These observations and the finding that LIN-35 is expressed broadly throughout development (Lu and Horvitz 1998) led us to hypothesize that: (1) *lin-35* must carry out additional functions during *C. elegans* development; and (2) the identification of such functions will necessitate the isolation of second-site mutations that interact synthetically with mutations in *lin-35* to produce novel phenotypes.

Using a nonbiased genetic approach, we have isolated a set of mutations that interact synthetically with *lin-35*. We report here the molecular identification and phenotypic characterization of one of these mutants, *fzr-1*, that affects the function of the *C. elegans* homolog of Cdh1/Hct1/Fizzy Related (FZR; Schwab et al. 1997; Sigrist and Lehner 1997; Visintin et al. 1997). In combination, mutations in *fzr-1* and *lin-35* lead to a striking hyperproliferation phenotype, showing for the first time that LIN-35 functions globally to control cell proliferation in *C. elegans*. In addition, we have also identified a synthetic requirement for *lin-35* and *fzr-1* during embryonic development, and describe an additional synthetic interaction between *lin-35* and the putative SCF complex (Skp1, Cullin, F-box) regulator, *lin-23* (Kipreos et al. 2000).

Results

A targeted strategy to identify novel lin-35 synthetic mutations

As a starting point for identifying novel *lin-35*/Rb synthetic mutants, we engineered strain MH1461 with two key components. The strain is (1) homozygous for a strong LOF mutation at the endogenous *lin-35* locus (*n745*) and (2) carries an extrachromosomal array (*kuEx119*) containing wild-type rescuing copies of *lin-35*

and a GFP reporter that is ubiquitously expressed (also see Materials and Methods). *kuEx119* fails to be transmitted to ~25% of progeny derived from *kuEx119$^+$* parents. Thus, *kuEx119$^+$* animals give rise to both *kuEx119$^+$* (*GFP$^+$/lin-35$^+$*) and *kuEx119$^-$* (*GFP$^-$/lin35$^-$*) progeny (Figs. 1 and 2A,B).

MH1461 animals were mutagenized and an F$_2$ clonal screen was carried out (also see Materials and Methods). Strains acquiring desirable mutations would be predicted to show clear-cut differences in the phenotypes of *kuEx119$^+$* and *kuEx119$^-$* progeny in the F$_3$ generation (Fig. 1). Through screening of ~3500 haploid genomes, we isolated seven mutations defining seven distinct loci. Animals homozygous for mutations in *lin-35* and the individual *slr* (synthetic with *lin-35*/Rb) genes show a range of phenotypes including reduced size, slow growth rates, larval lethality, and sterility (D.S. Fay and M. Han, unpubl.). As anticipated, the screen also uncovered a number of class A SynMuv mutations that were not further pursued. We describe here the phenotypic analysis and molecular identification of one *lin-35* synthetic mutation, *slr-1(ku298)*. Based on the molecular identity of the gene defined by this mutation (see below), we refer to this gene as *fzr-1*.

Synthetic interaction between lin-35 and fzr-1

In screening for *lin-35* synthetic mutants, we isolated candidate strain MH1621. MH1621 animals that carry *kuEx119* are healthy, fertile, and generally indistinguishable from wild-type animals. In contrast, *kuEx119$^-$* animals derived from this strain are nonviable and show multiple defects (Fig. 2C–F; see below). Genetic analyses indicated that the mutant phenotype observed in *kuEx119$^-$* progeny resulted from the combined effect of mutations in *lin-35* and a second unlinked gene, *fzr-1*.

As a further test for specificity, we inactivated *lin-35* using RNAi methods in strain MH1621. As expected, *lin-35(RNAi)* led to the highly penetrant expression of the *kuEx119$^-$* phenotype in *kuEx119$^+$* animals (Fig. 2G,H; see below), as a result of eliminating LIN-35 activity derived from the array. Based on these criteria, we conclude that the phenotype observed in MH1621 *kuEx119$^-$* progeny (hereafter referred to as *lin-35; fzr-1* double mutants) is the direct result of a synthetic interaction between *lin-35* and *fzr-1*.

fzr-1 single mutants isolated from strain MH1621 are viable and show no obvious anatomical or behavioral defects (see below). We did observe a low level of sterility in *fzr-1* hermaphrodites (3%, *n* = 104) as well as an ~50% reduction in brood size compared with wild type (142 ± 37, *n* = 8, vs. 264 ± 18, *n* = 50). In addition, *fzr-1* hermaphrodites produce males at an elevated frequency compared with wild type (1.74%, *n* = 1205, vs. ~0.2%; Sulston and Hodgkin 1988) and show an increase in the occurrence of embryonic lethality (11.9%, *n* = 1241, vs. <1%, *n* > 1000). An examination of *lin-35* single mutants revealed similar low levels of sterility (4%, *n* = 100) and embryonic lethality (6%, *n* = 382), as well as an ~65% reduction in brood size (98 ± 43, *n* = 10).
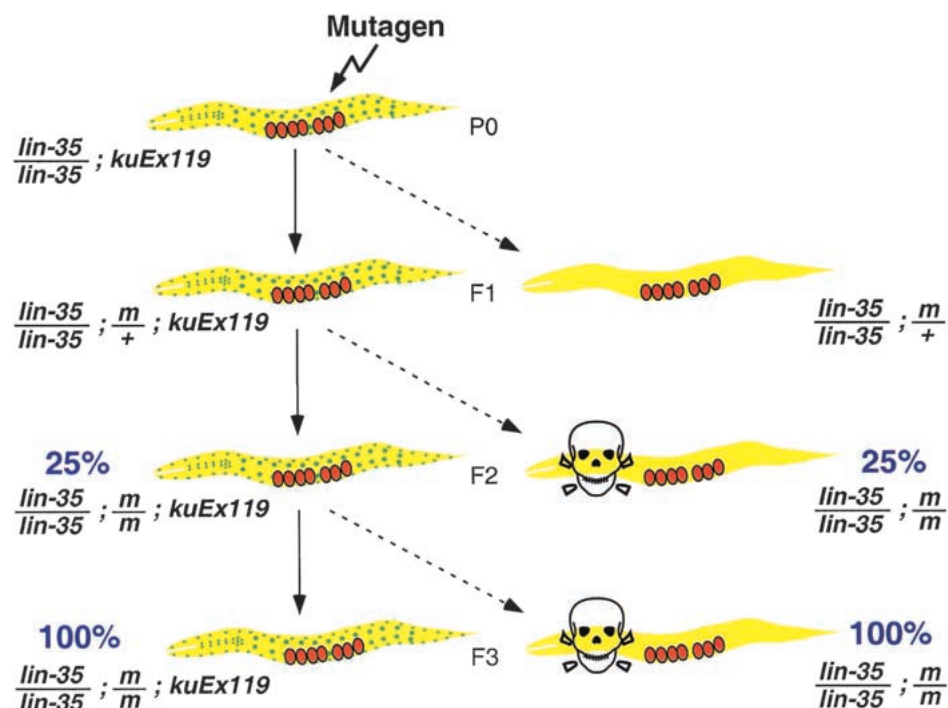
Figure 1. Outline of *lin-35* synthetic screen. Following chemical mutagenesis, three consecutive generations of *kuEx119⁺* animals are single-cloned and allowed to self-fertilize. Animals acquiring silent or otherwise viable mutations (*m*) that show synergy with *lin-35* are identified by the absence of wild-type-appearing *kuEx119⁻* progeny in the final (F₃) generation. Only animals carrying mutations are shown in subsequent generations. For further details, see text.

Whereas only 12% (n = 362) of *kuEx119⁺* animals derived from MH1621 fail to complete embryogenesis, 42% (n = 98) of sibling *lin-35; fzr-1* embryos fail to hatch, often arresting close to the end of elongation phase. For double mutants that successfully completed embryogenesis, the duration of embryonic development was similar to that observed for wild-type animals (~12–16 h). In contrast, the length of postembryonic development was greatly extended in *lin-35; fzr-1* animals, requiring 72 to >96 h at 20°C (n = 30) to complete larval stages versus 44 to 52 h (n = 200) for wild-type animals (Fig. 2C,D; data not shown). Adult *lin-35; fzr-1* animals show an approximate threefold reduction in total body volume compared with wild-type animals (Fig. 2E,F). In addition, some adult *lin-35; fzr-1* hermaphrodites produce small numbers of nonviable embryos, which remain within the uterus and show pleiotropic defects (Fig. 2E; data not shown; also see below).

lin-35; fzr-1 *double mutants show hyperproliferation in multiple tissue types*

An examination of *lin-35; fzr-1* double-mutant adults revealed extensive tissue hyperproliferation affecting subsets of cells derived from all the major germ layers (Sulston and Horvitz 1977). The supernumerary divisions appear to take place exclusively during postembryonic development as newly hatched *lin-35; fzr-1* L1 larvae show no evidence of excess cell divisions and are phenotypically indistinguishable from wild type (data not shown).

We measured the extent of hyperproliferation in three lineages derived from ectoderm in *lin-35* and *fzr-1* double mutants. Using a seam-cell-specific GFP marker (gift of J. Rothman, University of California, Santa Barbara), we observed up to a twofold increase in the number of hypodermal seam cells in *lin-35; fzr-1* double mutants and in *fzr-1* single mutants wherein *lin-35* was inactivated by RNAi (Table 1). Interestingly, normal numbers of seam cells were observed in *lin-35; fzr-1* double mutants derived from *lin-35* heterozygous hermaphrodites, indicating that *lin-35* maternal contributions are capable of suppressing hyperproliferation in at least some lineages (Table 1). Seam-cell proliferation was also normal in *lin-35* and *fzr-1* single mutants (Table 1).

Hyperproliferation was also observed in vulval tissue (Table 1; Fig. 3B) as well as in cells that make up the somatic gonad (data not shown). An analysis of vulval development revealed complex and variable defects in both induction and cell division patterns. This was owing in part to the presence of extra vulval precursor cells (VPCs) that were present in L2/L3 animals and were competent to respond to the induction signal. Induction of these supernumerary VPCs appeared to account for most or all of the extra vulval cells observed. VPC induction in *lin-35; fzr-1* mutants was dependent on *lin-3* signal: 13/38 *fzr-1; lin-3(e1417); lin-35(RNAi)* animals failed to produce any vulval tissue, similar to results
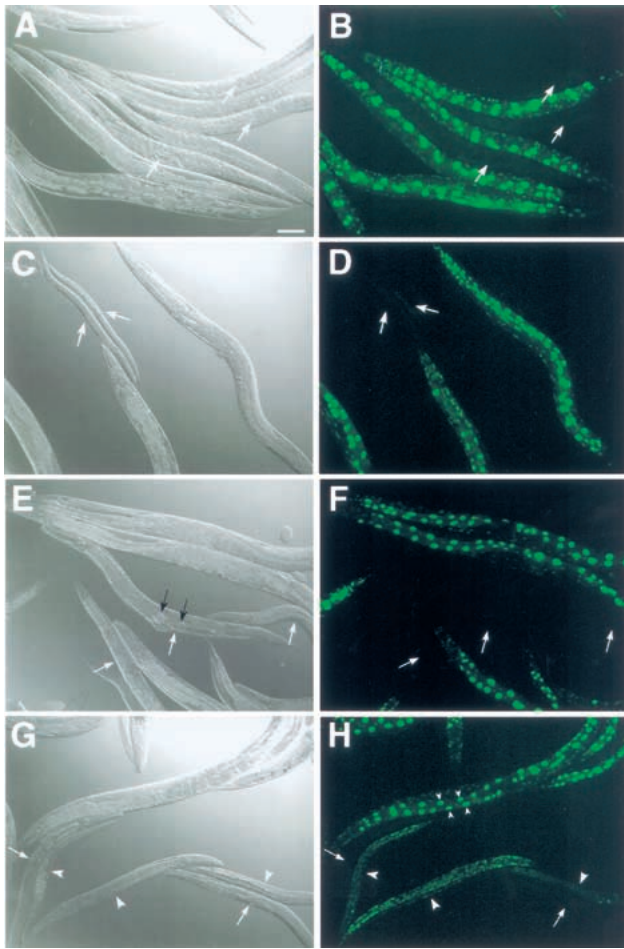
Figure 2. Synergism between *lin-35* and *fzr-1*. (*A,C,E,G*) DIC and corresponding (*B,D,F,H*) GFP fluorescence images. White arrows indicate positions of *kuEx119⁻* animals. (*A,B*) The starting strain for mutagenesis, MH1461 (*lin-35; kuEx119*). Note the identical appearance of *kuEx119⁺/⁻* adult animals. (*C–F*) *kuEx119⁺/⁻* progeny from strain MH1791 (*lin-35; fzr-1; kuEx119*), (*C,D*) ~60 h and (*E,F*) ~96 h posthatching. Note pronounced developmental-stage (*C,D*) and size (*E,F*) differences between *kuEx119⁺/⁻* animals. Black arrows indicate the location of nonviable embryos. (*D*) F₁ progeny of MH1791 animals injected with *lin-35* dsRNA (1.2 μg/μL). Large white arrowheads indicate the positions of *kuEx119⁺; lin-35(RNAi)* affected animals; small white arrowheads, GFP-expressing nuclei in untreated *kuEx119⁺* adults. Note the similar appearance of *kuEx119⁻* animals to *kuEx119⁺* animals affected by RNAi. Also note the absence of large GFP-expressing intestinal cells in the *kuEx119⁺* RNAi-affected animals. Size bar, 100 μm.

obtained for *lin-3(e1417)* mutants alone (10/21). Based on cell position assignments, the induced VPCs appeared to be derived exclusively from progenitor Pn.p cells that normally contribute to the vulva (P5.p, P6.p, and P7.p).

Following induction, VPCs underwent at least two to three rounds of divisions that were markedly slower and asynchronous compared with wild type. Whereas induced VPCs normally divide every 2 h, we often observed division times of >4 h and failed to observe accelerated division cycles. In addition, the pattern of vulval

cell fates based on division plane orientations and cell-fate-specific markers (*lin-11::GFP*) was highly variable (data not shown). These defects led to aberrant vulval morphologies; in some of these cases vulval cells failed to integrate into a single structure, producing multiple closely spaced invaginations reminiscent of a Muv phenotype (Fig. 3G,H).

In contrast to seam-cell and vulval lineages, ventral cord GABA neurons expressing *unc-47::GFP* (gift of E. Jorgensen, University of Utah, Salt Lake City) appeared to be completely unaffected in *lin-35; fzr-1* double mutants (Table 1). This absence of a phenotype may be due to the lack of a requirement for *lin-35* and *fzr-1* in controlling proliferation in these cells, or may result from suppression by maternal products of *fzr-1*.

Cells derived from the mesoderm were also affected, including distal-tip cells (DTCs), which guide migration of gonad arms during postembryonic development. *lin-35; fzr-1* double mutants showed a high frequency of ex-

Table 1. *Hyperproliferation of* lin-35; fzr-1 *double mutants*

|	Average cell no.	Range	n
Hypodermal seam-cell nuclei[a]			
Wild type	15.9 ± 1.2	14–19	25
lin-35	16.3 ± 0.9	15–18	8
fzr-1	16.5 ± 1.1	15–19	25
fzr-1; lin-35(RNAi)	21.2 ± 3.5	16–30	30
lin-35^{m+}; fzr-1^{m+}	17.1 ± 1.1	16–19	8
lin-35^{m+}; fzr-1	17.3 ± 1.5	16–21	17
lin-35; fzr-1^{m+}	23.2 ± 2.5	18–26	9
Vulval cell nuclei			
Wild type	22.0 ± 0.0		>100
lin-35	22.0 ± 0.0		20
fzr-1	22.0 ± 0.0		20
lin-35; fzr-1	30.6 ± 5.8	22–43	13
***unc-47::GFP*-expressing GABA neurons[b]**			
Wild type	18.4 ± 0.8	17–19	12
lin-35^{m+}; fzr-1^{m+}	18.9 ± 0.8	18–20	12
lin-35^{m+}; fzr-1	18.4 ± 0.7	17–19	7
lin-35; fzr-1^{m+}	18.1 ± 0.9	17–19	10
fzr-1; lin-35(RNAi)	18.5 ± 0.7	17–19	20
Intestinal cell nuclei[c]			
Wild type	26.3 ± 0.4	20–32	43
fzr-1	35.8 ± 1.5	23–48	21
lin-35(RNAi)	29.0 ± 0.7	20–39	43
fzr-1; lin-35(RNAi)[d]	52.2 ± 7.1	44–67	20

Cell numbers were scored for wild-type and mutant animals either directly (vulval cells) or using cell-type-specific integrated GFP markers.
[a]Hypodermal seam cells were scored using a seam-cell-specific GFP marker strain, JR632. *m+* indicates the presence of maternal gene product.
[b]*unc-47::GFP*-expressing GABA neurons were assayed using a GFP marker strain, *oxln12*. Only those cells located between the rectum and pharyngeal grinder were scored.
[c]Intestinal cells were scored using an *elt-2::GFP* marker strain.
[d]Owing to weak and variable GFP staining in *fzr-1; lin-35(RNAi)* animals, numbers obtained are likely to be underestimates of the total number of intestinal cells (also see text).
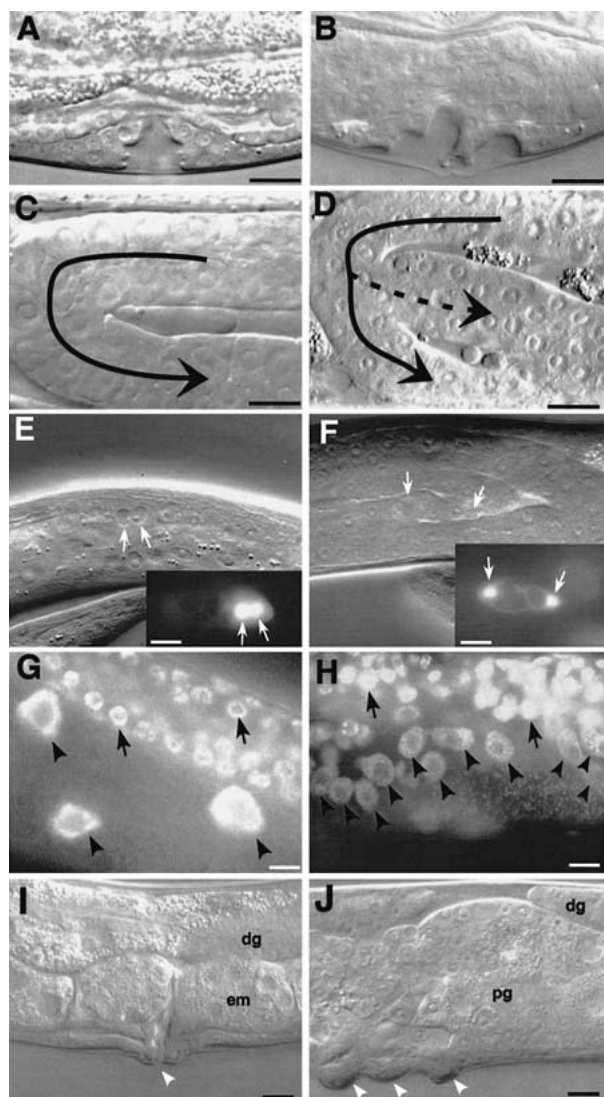
Figure 3. Hyperproliferation of *lin-35; fzr-1* double mutants. (*A,C,G,I*) *lin-35; fzr-1; kuEx119* and (*B,D,H,J*) *lin-35; fzr-1* animals. (*A,B*) L4-stage vulvae. The vulva in *A* contains 22 nuclei and is indistinguishable from wild type, whereas the vulva in *B* contains 32 nuclei and shows an abnormal morphology. (*C,D*) Morphology of the gonad arm in L4/young-adult animals. The gonad arm in *C* appears completely wild type whereas that in *D* contains a single bifurcation, the result of an extra division of the distal tip cell. (*E,F*) Distal tip cells (arrows) in *fzr-1; lin-35(RNAi)* animals expressing *lag-2::GFP*. The DTCs in *E* are in the process of dividing whereas *F* shows cells several hours after divisions have taken place. The images in *E* and *F* are of different animals. (*G,H*) DAPI staining of intestinal (arrowheads) and distal germ (arrows) cells. Contrast the large, brightly staining intestinal cells in *G* to the smaller, fainter intestinal cells in *H*. A relative indication of intestinal-cell DNA content can be inferred from comparing the intensity of intestinal-cell staining to that of the germ cells in each panel. (*I,J*) Proximal gonad and vulval region in adults. White arrowheads indicate the location of vulval eversions. Note the presence of multiple eversions in *J*. In addition, the animal in *J* shows a hyperproliferation defect of the proximal germ line (pg), whereas the animal in *G* contains wild-type embryos (em) in this region. The distal germ line (dg) appears normal in both *I* and *J*. Size bars, 10 μm.

tra DTCs, leading to a Shiva (Shv) phenotype, in which an abnormal bifurcation produces gonads with extra arms (Fig. 3C,D; Table 2). In general, only one bifurcation per gonad arm was observed, indicating that most DTCs were undergoing only a single extra division cycle. Consistent with this, the average number of DTCs detected using the DTC-expressing *lag-2::GFP* marker (Blelloch et al. 1999) was 1.67 ± 0.68 (range, 1–4; $n = 60$) per gonad arm, where only 5/60 animals contained >2 DTCs per arm. An analysis of DTC divisions in *fzr-1; lag-2::GFP; lin-35(RNAi)* animals indicated that most or all extra DTCs are generated through division of the DTC itself, and not from other cell types in the somatic gonad. This result was supported by the direct observation of *lag-2::GFP*-expressing DTCs in the process of division (Fig. 3E,F), and by experiments where DTCs were laser-ablated in L2-stage animals: 6/7 animals failed to produce additional DTCs based on gonad morphology and *lag-2::GFP* expression. This result contrasts with findings in *cki-1(RNAi)* animals where supernumerary DTCs were shown to originate from other cells within the somatic gonad (Hong et al. 1998). We cannot, however, rule out the possibility that a small percentage of DTCs in *lin-35; fzr-1* animals may be derived from other sources.

Endoderm was also strongly affected in *lin-35; fzr-1* double mutants. Wild-type adults normally contain ~26 gut cell nuclei that are polyploid (32N) as a consequence of four endoreduplication cycles (DNA replication without intervening mitosis) during larval development (Fig. 3G; Hedgecock and White 1985). In *lin-35; fzr-1* double mutants, gut cell ploidy was highly variable, ranging from 2N to 16N ($n = 20$), with the majority of cells falling in the range of 4N to 8N (Fig. 3H; data not shown). In

Table 2. fzr-1 *genetic interactions with SynMuv genes*

	% Shv	n
lin-35(n745)	1	76
fzr-1(ku298)	0	40
lin-35; fzr-1; kuEx119	2	97
lin-35; fzr-1	58	45
lin-35; fzr-1; kuEx119; lin-35(RNAi)[a]	68	60
lin-35; fzr-1; kuEx119; lin-36(RNAi)[a]	69	36
lin-35; fzr-1; kuEx119; efl-1(RNAi)[a]	46	26
fzr-1; lin-53(n833)	0	25
lin-35; fzr-1; kuEx119; lin-53(RNAi)[b]	4	28
lin-35; fzr-1; kuEx119; hda-1(RNAi)[b]	0	25
lin-35; fzr-1; kuEx119; chd-4(RNAi)[b]	0	43
fzr-1; lin-15a(n767)	0	22
lin-35; fzr-1; kuEx119; lin-15a(RNAi)	7	81
lin-35; kuEx119; fzr-1(RNAi)	2	61
lin-35; fzr-1(RNAi)	37	49

Adult hermaphrodites of the indicated genotypes were placed on RNAi feeding plates, and adult F$_1$ progeny were scored for the presence of the Shiva (Shv) phenotype. *kuEx119* is the extrachromosomal array containing the *lin-35+* gene.
[a]Similar percentages of Shv animals were also observed following RNAi treatment of *fzr-1* single mutants.
[b]RNAi treatment led to a highly penetrant sterile phenotype among F$_1$ progeny.

addition, we observed *lin-35; fzr-1* DAPI-stained animals that contained up to four times the normal number of intestinal cell nuclei (Fig. 3H). Consistent with this, *fzr-1; lin-35(RNAi)* animals expressing the gut-cell-specific marker *elt-2::GFP* showed excess divisions (Table 1). The large number and reduced ploidy of mutant gut cells suggest that rather than executing endocycles during larval development, intestinal cells in the double mutants are undergoing cycles of DNA replication followed by mitosis. Interestingly, both *lin-35* and *fzr-1* single mutants showed a modest increase in the number of gut cell nuclei compared with wild type (Table 1).

Excess divisions were also observed in cells that make up the germ line. Severe effects were confined to proximal regions of the gonad, where rampant hyperproliferation led in some cases to a tumorous phenotype (Fig. 3I,J; Francis et al. 1995). The specific involvement of germ cells was evidenced by the lack of any detectable GFP expression in affected regions of the gonad in MH1621 animals in which *lin-35* was inactivated with RNAi (data not shown). This failure of the tumorous cells to express GFP reflects the ability of germ-line cells to efficiently silence transgene expression, a characteristic not associated with the somatic gonad, in which we observed consistent GFP expression. Distal gonad regions were less affected and showed normal-appearing DAPI-stained mitotic, transition, and pachytene zones (data not shown). These results suggest that germ cells in *lin-35; fzr-1* mutants abnormally reenter mitosis after failing to progress past meiotic prophase. These defects could reflect a direct requirement for *lin-35* in germ cells, or may be caused by nonautonomous effects, such as signaling via the *lag-2/glp-1* pathway from the somatic gonad.

fzr-1 *shows synthetic phenotypes with a subset of class B SynMuv genes*

As described in the introduction, a subset of class B SynMuv genes (including *lin-35*) have been linked to transcriptional regulation. However, it is currently unclear to what extent these functionally related genes are interchangeable with respect to their genetic interactions. To address this issue, we examined interactions between *fzr-1* and six SynMuv genes. The class B genes *efl-1*, *lin-53*, *hda-1*, and *chd-4* encode homologs of E2F (Ceol and Horvitz 2001), RbAp48, histone deacetylase (Lu and Horvitz 1998), and the NuRD complex component, Mi-2, respectively (Solari and Ahringer 2000; von Zelewsky et al. 2000). *lin-15a* and *lin-36* (class A and B genes, respectively) encode novel proteins (Clark et al. 1994; Huang et al. 1994; Thomas and Horvitz 1999).

Similar to the effects observed for *lin-35(RNAi)* (Fig. 2G,H; Tables 1, 2), RNAi inactivation of either *lin-36* or *efl-1* in strain MH1621 led to the appearance of *kuEx119*[+] animals that were phenotypically indistinguishable from *lin-35; fzr-1* double mutants (Table 2; data not shown). In contrast, RNAi inactivation of *lin-53*, *hda-1*, *chd-4*, and *lin-15a* failed to induce hyperproliferation in *kuEx119*[+] animals (Table 2; data not shown).

In addition, we constructed double mutants between *fzr-1* and *lin-53* and *lin-15a*. In both cases, double-mutant animals were indistinguishable from wild type with respect to viability and cellular proliferation properties (Table 2; data not shown). We conclude that *fzr-1* shows interactions with a subset of class B genes that may function more specifically to control cell cycle regulation.

fzr-1 *encodes a* C. elegans *homolog of Cdh1/Hct1/FZR*

Using several novel approaches to overcome a number of technical challenges (see Materials and Methods), we mapped *ku298* to a small region on LGII between *let-23* and *unc-4*. We attained rescue of the *lin-35; fzr-1* double-mutant phenotype using microinjection with a single cosmid from the region ZK1307. Partial but clear rescue was subsequently obtained with a subclone of ZK1307 that contained only a single predicted ORF, ZK1307.6 (see Materials and Methods). A search of the database indicated that ZK1307.6 encodes the *C. elegans* homolog of Cdh1/Hct1/FZR.

To further support the claim that *ku298* represents an allele of *fzr-1*, we sequenced *fzr-1* genomic DNA from *ku298* mutant animals. We detected a single missense mutation within the predicted coding region of *fzr-1*. The mutation (G → A) substitutes a highly conserved cysteine with tyrosine in the fourth WD-repeat domain (Fig. 4A). As an additional test, strain MH1461 was grown on *fzr-1(RNAi)* feeding plates. Although *kuEx119*[+] animals appeared largely unaffected by this treatment, the majority of *kuEx119*[−] animals showed hyperproliferation defects similar to those of *lin-35; fzr-1* double mutants (Fig. 5A; Table 2; data not shown).

Using a cDNA clone (gift of Y. Kohara, National Institute of Genetics, Mishima, Japan), we confirmed the predicted gene structure of *fzr-1* and identified an SL1 transplice leader sequence (Krause and Hirsh 1987) at the 5′ end of the clone, indicating that it is full length. The highly conserved C-terminal domain of FZR-1 is 68% identical to both *Drosophila* FZR and human CDH1 (Fig. 4A). The sizable N-terminal domain of FZR-1 contains scattered regions of homology to the fly and human gene products as well as novel sequences (Fig. 4A). A phylogenetic analysis indicates that FZR-1 is more similar to members of the Cdh1/Hct1/FZR family than to the closely related but functionally distinct gene family composed of Cdc20/FZY (Fig. 4B).

FZR-1 *function is required for fertility*

The nature of the genetic lesion suggested that *ku298* might not represent a complete LOF allele of *fzr-1*. Because dsRNA injection techniques may produce RNAi phenotypes that more closely mimic that of the molecular null than do those produced by feeding methods (M. Han, unpubl.), we inactivated FZR-1 function in wild-type animals using RNAi injection methods. Injection led to a severe reduction in the fertility of the de-

rived F$_1$ progeny: 47% of F$_1$ animals were completely sterile, whereas an additional 39% had brood sizes of <10 (n = 210). An analysis of affected animals revealed pleiotropic defects within the germ-line and somatic gonad. These included a failure of gonad arms to elongate, missing or abnormal oocytes and sperm, and morphogenetic defects of the uterus and vulva (Fig. 5B; data not shown). From these results, we conclude that FZR-1 function is required for viability and that *ku298* encodes a hypomorphic allele of *fzr-1*.

We also examined the effect of inactivating *fzr-1* using RNAi injection methods in a *lin-35* mutant background. Interestingly, this led to embryonic lethality in 88% of F$_1$ progeny, with the remaining 12% arresting during early larval stages (n = 269). Nonviable embryos showed a variety of phenotypes ranging from premorphogenetic to late-stage arrest (Fig. 5C,D). In the majority of cases, arrested embryos showed clear signs of tissue-specific differentiation but failed to complete morphogenesis and contained vacuoles and necrotic regions (Fig. 5C,D). In addition, a significant percentage of embryos (~30%) were misshapen or of abnormal size (Fig. 5D). We conclude that, in addition to controlling cell proliferation during postembryonic development, *lin-35* and *fzr-1* play essential, albeit redundant, roles during embryonic development.

Consistent with these findings, an *fzr-1::GFP* transcriptional reporter showed robust expression in most or all cells during embryonic development in wild-type animals (Fig. 5E,F). Expression was also observed at lower levels in many cell types during larval development, including those showing proliferation defects in *lin-35; fzr-1* double mutants (data not shown).

lin-35 *shows a synthetic interaction with the putative SCF regulator* lin-23

lin-23 encodes a WD-repeat protein with homology to regulators of the SCF proteosome complex (for review, see Deshaies 1999; Kipreos et al. 2000). Loss of LIN-23 function leads to a widespread hyperproliferation phenotype in mutant animals, presumably resulting from a failure to degrade G$_1$ cyclins. We had previously identified an allele of *lin-23* in an earlier screen for *lin-35* synthetic mutants (D.S.F. and M.H., unpubl.). *lin-23(ku294)* contains a mutation in the conserved 5′ splice site (GT → AT) between exons 4 and 5 of *lin-23*, resulting in a peptide that is predicted to terminate following amino acid 245 of the 665-amino-acid peptide. Based on the size of the truncation and the predicted instability of the resulting mRNA, *ku294* is likely to represent a strong or complete LOF allele of *lin-23*.

In contrast to *lin-23* and *lin-35* single mutants, *lin-35; lin-23(ku294)* double mutants generally fail to progress past the L3 larval stage and are severely growth retarded relative to the single mutants (Fig. 6A; data not shown). Because of the extremely poor viability of *lin-35; lin-23* double mutants, and the fact that *lin-23* single mutants themselves show a strong hyperproliferation phenotype on their own, it was not possible for us to discern whether the absence of LIN-35 function exacerbated the *lin-23* hyperproliferation defect in the double mutants.

As an alternative approach, we reduced *lin-23* function in MH1461 animals using RNAi feeding methods and looked for differences in the sensitivity of *lin-35; kuEx119$^+$* and *lin-35; kuEx119$^-$* sibling progeny. Interestingly, whereas 82% (n = 177) of *kuEx119$^-$* animals exposed to *lin-23(RNAi)* showed the characteristic *lin-23* hyperproliferation phenotype, only 43% (n = 236) of sibling *kuEx119$^+$* animals were similarly affected (Fig. 6B,C). Thus the presence of functional LIN-35 significantly decreased sensitivity to diminished LIN-23 activity. This effect was not due to a generic hypersensitivity of *lin-35* mutant animals to RNAi as both *kuEx119$^+$* and *kuEx119$^-$* animals were equally sensitive to *unc-22(RNAi)* feeding (data not shown).

LIN-35 and FZR-1 likely coregulate G$_1$ cyclin levels

Based on work from other systems (see Discussion), loss of LIN-35 function would be predicted to disrupt the activity of Rb/E2F transcriptional inhibitory complexes, leading to elevated levels of cyclin E and cyclin A mRNA. In turn, loss of either FZR-1 or LIN-23 would result in decreased APC or SCF functions, leading to an increase in the stability of cyclin A and cyclin E proteins, respectively. A simple model would then predict that in the *lin-35; fzr-1* double mutant, the combination of both increased cyclin transcription and stability leads to cyclin protein levels that are sufficient to override the normal G$_1$ arrest.

To test this model, we engineered strains containing temperature-inducible cyclin A or cyclin E constructs expressed from extrachromosomal arrays. As shown in Table 3, in an otherwise wild-type background, either cyclin A or cyclin E overexpression can lead to the production of extra distal tip cells in a small percentage of animals. Notably, this effect is strongly enhanced in an *fzr-1* mutant background. The synthetic interaction observed between cyclin overexpression and *fzr-1* mutants is consistent with the model that LIN-35 and FZR-1 cooperate to control the levels of G$_1$ cyclins through transcriptional repression and protein destabilization, respectively.
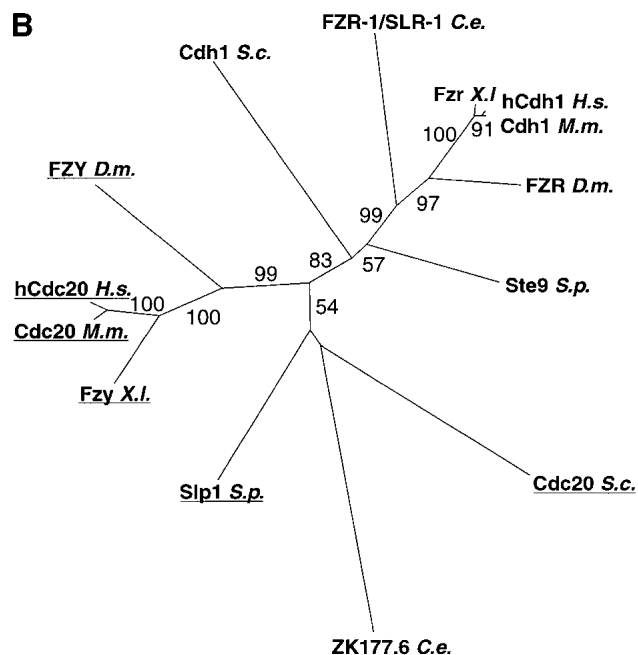
Discussion

lin-35 *and the control of cell proliferation*

We report here the cloning and characterization of *fzr-1*, a gene that cooperates with *lin-35* to control cell proliferation. A relatively small number of genes have been described that cause widespread hyperproliferation in *C. elegans*. These include the putative SCF components *cul-1* and *lin-23* (Kipreos et al. 1996, 2000), the CIP/KIP family member *cki-1* (Hong et al. 1998), and the CBP/p300 homolog *cbp-1* (Shi and Mello 1998). In the cases examined thus far, a hyperproliferation phenotype is observed following inactivation of a single gene product.

A

(*Figure 4 continued on facing page*)

We have shown that loss of cell proliferation control can also result from a synthetic genetic interaction. Although single mutants of *lin-35* and *fzr-1* showed only subtle or low-penetrance phenotypes, *lin-35; fzr-1* double mutants showed extensive tissue hyperproliferation affecting a wide range of cell types (Figs. 3–5; Tables 1, 2). Thus, uncontrolled proliferation in *C. elegans* can in essence follow the same genetic pattern as multistep car-

Figure 4. (*A*) Peptide alignment of *C. elegans* FZR-1, *Drosophila melanogaster* Fzr, and *Homo sapiens* CDH1. Black boxes signify identity; gray, similarity. The boundaries of the seven WD-repeat regions are indicated by arrows and corresponding numbers. The location of the *ku298* lesion is indicated by an asterisk. (*B*) Unrooted phylogenetic tree diagram showing relationships between FZR (non-underlined) and FZY (underlined) homologs from *C. elegans*, *D. melanogaster*, *Xenopus laevis*, *Mus musculus*, *H. sapiens*, *Saccharomyces cerevisiae*, and *Schizosaccharomyces pombe*. Numbers indicate bootstrap values.

cinogenesis in mammals. Namely, proliferation control is abolished through the sequential loss of genes that function to restrain cell cycle progression.

Given our findings, and the large body of evidence implicating *Rb* in human cancers (for review, see Nevins 2001), it seems reasonable to suggest that our technical approach may facilitate the study of multistep carcinogenesis using *C. elegans*. Along these lines, it will be interesting to determine whether the human homolog of *fzr-1*, hCDH1, can function as a tumor-suppressor gene, and if so, whether it does so in cooperation with Rb.

Inactivation of *fzr-1* function using RNAi injection led to sterility and aberrancies in germ cell proliferation (Fig. 5A,B). Although we have not determined the specific cause of this phenotype, previous studies would implicate defects in either the execution of G_1 arrest (Irniger and Nasymth 1997; Sigrist and Lehner 1997; Zachariae et al. 1998) or in late-stage mitotic events such as cytokinesis (Schwab et al. 1997; Zur and Brandeis 2001). We also observed embryonic lethality when *fzr-1* was inactivated using RNAi injection in a *lin-35* mutant background (Fig. 5C,D). The cause for this lethality is presently unknown. These embryos do not show obvious hallmarks associated with either excess cellular proliferation or grossly elevated levels of apoptosis (data not shown). Although additional work will be necessary to determine the nature of this embryonic requirement, a role during embryonic development is consistent with the expression patterns observed for both *fzr-1* (Fig. 5E,F) and *lin-35* (Lu and Horvitz 1998). The lack of an apparent hyperproliferation phenotype in embryos likely reflects significant differences in the means by which embryonic and postembryonic cell cycles are regulated. For example, cyclin D, an upstream regulator of Rb, has been shown to be required exclusively for the execution of postembryonic division cycles in *C. elegans* (Park and Krause 1999; Boxem and van den Heuvel 2001).

Differential properties of SynMuv genes

Work carried out over the past several years has produced an explosion in the number of identified SynMuv genes (see Fay and Han 2000). Although certain functional classifications, such as transcriptional repressors, may accurately describe some of the SynMuv genes, others clearly defy straightforward categorization. This fact alone suggests that SynMuv genes most likely do not all act through the same mechanisms or pathways.

We have found that both *lin-36* and *efl-1(RNAi)* can phenocopy the effect of *lin-35* LOF in an *fzr-1* mutant background (Table 2). However other class B genes, including *lin-53*, *hda-1*, and *chd-4*, did not show genetic interactions with *fzr-1*, nor did the class A gene *lin-15a* (Table 2). These experiments are complicated by the fact that *lin-53*, *hda-1*, and *chd-4* encode for essential genes, and RNAi leads to a highly penetrant sterile or lethal phenotype within several generations. Nevertheless, we saw no evidence for hyperproliferation in either the affected or unaffected classes of RNAi-treated animals. This suggests that neither a weak nor a severe reduction in the function of these genes is capable of producing a synthetic hyperproliferation phenotype with *fzr-1*. In addition, we detected no evidence for an interaction in *lin-53(n833); fzr-1* double-mutant animals. Although *n833* results in only a partial loss of LIN-53 function (Lu and Horvitz 1998), this allele does lead to a highly penetrant Muv phenotype in conjunction with class A SynMuv mutations (Ferguson and Horvitz 1989).

These data indicate a functional distinction between those class B genes that may play relatively direct roles in the regulation of the cell-cycle machinery (*lin-35*, *lin-36*, and *efl-1*) and others that may function more generally in the regulation of chromatin modification and transcriptional control (*lin-53*, *hda-1*, and *chd-4*). Moreover, our data correlate well with recent studies on vulval-cell fate specification, in which clear functional differences were observed between similar subsets of class B genes (Chen and Han 2001).

lin-35, fzr-1, lin-23, and cyclin regulation

Rb and its family members p107 and p130 have been shown in multiple systems to modulate transcription through direct interactions with a variety of transcrip-
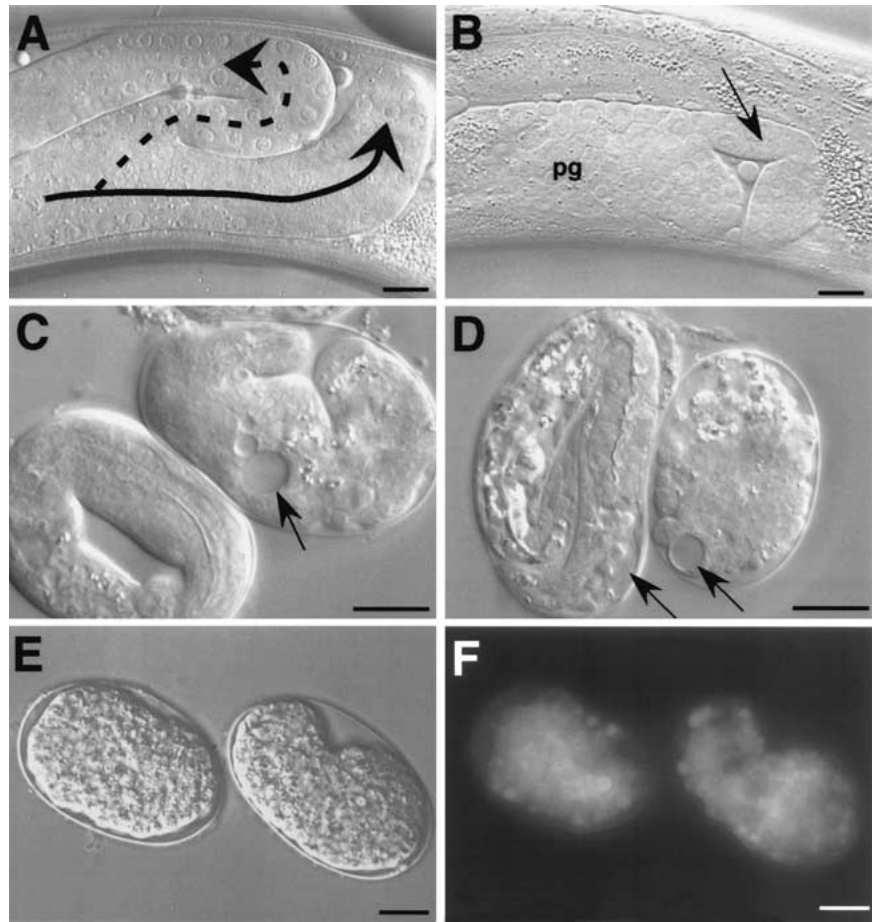
Figure 5. *fzr-1(RNAi)* and *fzr-1* expression. (*A*) Example of the Shv phenotype observed in *lin-35* animals grown on *fzr-1(RNAi)* feeding plates. (*B*) Representative gonad from progeny of N2 animals injected with *fzr-1* dsRNA (RNAi; 1.5 µg/µL). Note the small malformed gonad arm extension (arrow) protruding from the proximal gonad region (pg). (*C,D*) Terminal embryos derived from *lin-35* animals injected with *fzr-1* dsRNA. Arrows indicate the locations of vacuoles. Note the variability in embryonic (*C,D*) arrest point and (*D*) size. (*E,F*) Corresponding DIC and GFP fluorescence images of an *fzr-1::GFP* reporter construct expression in wild-type embryos. Size bars, 10 µm.

tional regulators (for review, see Kaelin 1999; Zheng and Lee 2001). The majority of work indicates that Rb serves primarily as a transcriptional repressor, acting through a number of mechanisms including the recruitment of chromatin-modifying enzymes (Dunaief et al. 1994; Brehm et al. 1998; Luo et al. 1998; Magnaghi-Jaulin et al. 1998; Zhang et al. 2000; Nielsen et al. 2001) and the steric interference of transactivation domains (Flemington et al. 1993; Helin et al. 1993; Weintraub et al. 1995). Acting as transcriptional corepressors with E2F (for review, see Dyson 1998; Harbour and Dean 2000; Classon and Dyson 2001), Rb and its family members regulate the expression of many key genes required for entry and progression through S-phase (Dou et al. 1994) including cyclin E (DeGregori et al. 1995; Duronio and O'Farrell 1995; Ohtani et al. 1995) and cyclin A (Degregori et al. 1995; Schulze et al. 1995). Consistent with these reports, we have observed a significant increase in the levels of ribonucleotide reductase mRNA, an E2F-regulated gene, in *lin-35* mutant animals (D.S. Fay and M. Han, unpubl.).

In contrast, Cdh1/Hct1/FZR and its close relative Cdc20/FZY function as regulatory subunits for the anaphase-promoting complex (APC) cyclosome (Dawson et al. 1995; Sigrist et al. 1995; Schwab et al. 1997; Visintin et al. 1997; for review, see Morgan 1999; Zachariae and Nasmyth 1999). This multisubunit peptide complex is thought to function as a ubiquitin ligase, and targets the degradation of several key factors during mitosis, including yeast Pds1 (Cohen-Fix et al. 1996), human securin/PTTG (Zur and Brandeis 2001), and cyclins A and B in higher eukaryotes (Dawson et al. 1995; Irniger et al. 1995; King et al. 1995; Sigrist et al. 1995; Sudakin et al. 1995). APC function requires activation first by Cdc20/FZY during metaphase/anaphase, and then by Cdh1/Hct/FZR during late mitosis and G_1. It is believed that Cdh1 and Cdc20 differentially target distinct but overlapping subsets of proteins for degradation by the APC cyclosome (see above references; for review, see Morgan 1999; Zachariae and Nasmyth 1999).

In *Drosophila*, loss of *fzr* function leads to reentry into the cell cycle following embryonic cycle 16, thereby bypassing the normal G_1 arrest (Sigrist and Lehner 1997). This ectopic division cycle is correlated with excess levels of cyclin A (Sigrist and Lehner 1997), which when overexpressed during G_1 can lead to ectopic entry into S-phase (Sprenger et al. 1997). Interestingly, mutations in the *Drosophila* Rb homolog *rbf* (Du and Dyson 1999), as well as in the CDK inhibitor *decapo* (de Nooij et al. 1996), show cell cycle defects similar to those of *fzr* mutants, suggesting complementary roles in G_1/S-phase regulation. However, we note that conclusions regarding *fzr* functions were inferred from the analysis of a large
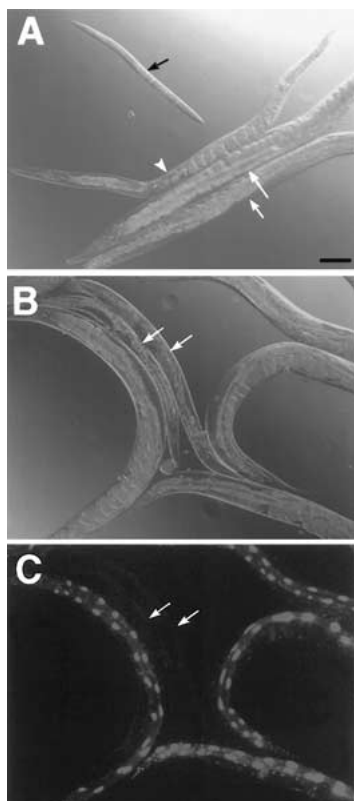
Figure 6. *lin-35; lin-23* synthetic interactions. (*A*) *lin-35* single mutant (white arrows), *lin-23(ku294)* single mutant (white arrowhead), and *lin-35; lin-23* double mutants (black arrow). The *lin-35; lin-23* animal shown is >96 h posthatching and shows the typical midlarval-stage terminal arrest phenotype. (*B,C*) Corresponding DIC and GFP fluorescence images of representative adult MH1461 animals propagated on *lin-23(RNAi)* feeding plates. White arrows indicate the positions of *Ex119⁻* animals. Note the preferential effect of *lin-23(RNAi)* on the *kuEx119⁻* animals. Size bar, 100 μm.

deletion that removed several genes in addition to *fzr* (Sigrist and Lehner 1997). Therefore, *fzr-1(ku298)* is the first reported mutation in metazoans that specifically reduces CDH1/HCT1/fzr activity.

Our analysis of DTC hyperproduction in strains that overexpress either cyclin A or cyclin E mRNA (Table 3) supports the model that *lin-35* and *fzr-1* are likely to coregulate cyclin levels during G$_1$. In addition, our finding that the E2F homolog *efl-1* synergizes with *fzr-1* (Table 2) adds further credence to this model. The ability of both cyclin A and cyclin E to induce extra DTCs in *fzr-1* mutants could indicate that these cyclins may be functionally interchangeable and that sufficient levels of either cyclin A or cyclin E, or possibly both in combination, can work to override G$_1$ arrest.

Multiple mutations show synthetic lethality with lin-35

By screening ~3500 haploid genomes, we uncovered seven Slr mutations that show synthetic lethality or in-

viability with mutations in *lin-35*. The phenotypes observed in the double mutants range from embryonic and early larval arrest to adult sterility and size defects (D.S. Fay and M. Han, unpubl.). About half of the Slr mutations that we have identified show only little or no phenotype as single mutants, whereas others show moderate effects on brood size and/or growth rates. In addition, we note that the penetrance and severity of the double-mutant phenotypes appear in several cases to be substantially reduced by the presence of low levels of maternal *lin-35* expressed from the array, consistent with previous reports that maternal *lin-35* can also suppress expression of the Muv phenotype (Ferguson and Horvitz 1989).

Other than *fzr-1* and *lin-23*, we have not yet identified any Slr mutations that produce an obvious synthetic hyperproliferation phenotype with *lin-35*. However, as inferred from our comparison of *lin-35(n745); fzr-1(ku298)* and *lin-35(n745); fzr-1(RNAi)* phenotypes, this may depend to a significant extent on the specific nature of the allele isolated. Therefore, whether or not additional Slr genes will turn out to function in cell cycle control mechanisms or will cooperate with *lin-35* in activities not directly related to the cell cycle remains to be seen.

A screen of general utility

We believe the means used to uncover the genetic interaction between *lin-35* and *fzr-1* will be of general use for those wishing to assign functions to genes lacking known biological roles or to identify novel functions for genes with previously characterized activities. In addi-

Table 3. *Heat shock of cyclin A and cyclin E*

	% Shv	*n*
Cyclin A overexpression		
fzr-1; (fdEx1)	16	154
fzr-1	0	91
N2; (*fdEx1*)	5	78
N2	0	70
fzr-1; (fdEx2)	32	122
fzr-1	1	69
N2; *fdEx2*	5	86
N2	0	63
Cyclin E overexpression		
fzr-1; (fdEx6)	18	122
fzr-1	0	115
N2; (*fdEx6*)	3	64
N2	0	42
fzr-1; (fdEx7)	5	124
fzr-1	1	127
N2; (*fdEx7*)	1	62
N2	0	50

Strains harboring cyclin A (*fdEx1, fdEx2*) or cyclin E (*fdEx6, fdEx7*) heat-shock expression constructs contained on extrachromosomal arrays were generated as described in Materials and Methods. Mixed-stage L1/L2 larval animals were heat-shocked at 33°C for 4 h and allowed to recover at 20°C for ~52 h. Sibling *Ex⁺/Ex⁻* young adult animals were then analyzed for the Shiva phenotype. Percentages indicate the averages obtained from two separate experiments.

tion, this genetic approach serves to identify functional copartners through the isolation and cloning of the affected second-site mutations. Importantly, this method in no way depends on prior knowledge of the synthetic double-mutant phenotype, thereby permitting a nonbiased search for genetic modifiers of any gene of interest.

Given the inevitable saturation of the genome for mutations that cause easily detectable phenotypes, the ability to identify synthetic mutations will become increasingly important. Large-scale analyses carried out in yeast and *C. elegans* suggest that a large percentage of genes in higher organisms may fail to show easily discernable phenotypes when mutated (Smith et al. 1996; Winzeler et al. 1999; Fraser et al. 2000). It is likely that the vast majority of these no-phenotype genes may nevertheless confer a weak selective advantage to the organism, thus accounting for their presence in the genome (Nowak et al. 1997; for review, see Tautz 2000). At the same time, it can be argued that many of these genes fail to show mutational effects owing to genetic redundancy. Importantly, these two explanations are in no way mutually exclusive. By devising methods to experimentally address this latter issue, we may hope to assign biological roles to many genes that would normally not be amenable to straightforward functional analyses.

Materials and methods

Culture methods

Maintenance, culturing, and genetic manipulations of *C. elegans* strains were carried out according to standard procedures (Sulston and Hodgkin 1988) and conducted at 20°C.

Strains used/generated

The strains used or generated were as follows: MT1624 [*lin-35(n745)I; lin-8(n111)II*], MH1461 [*lin-35(n745)*I; kuEx119], MH1621 [*lin-35(n745)I; fzr-1(ku298)II; kuEx119*], MH1829 [*fzr-1(ku298), unc-4(e120)II*], MH1832 [*dpy-10(e128), fzr-1(ku298), unc-4(e120)II*], CB4856, MH1791 [*fzr-1(ku298)II*], MH1640 [*lin-35(n745)I; dpy-10(e128), unc-4(e120)II*], MH1630 [*lin-35(n745)I; bli-2(e768), rol-6(e187)II*], MH1758 [*lin-35(n745)I; let-23(sy15), unc-4(e120)/dpy-10(e128), unc-4(e120)II*], JK2533 [*qC1(lag-2::GFP qIs26)/eT1* (Blelloch et al. 1999)], GR1314 [*mgIs21 (lin-11::GFP* (Hobert et al. 1998)], JR632 [seam cell::GFP (Terns et al. 1997)], oxIn12 [*unc-47::GFP* (McIntire et al. 1997), and JM63 [*elt-2*::GFP (Fukushige et al. 1998)].

DNA constructs

RNAi Target sequences for insertion into pPD129.36 (gift of A. Fire) were generated by PCR amplification from appropriate cDNA or genomic clones. cDNA clones of *lin-35*, *efl-1*, *lin-36*, *hda-1*, and *lin-53* were obtained from Y. Kohara, and a cDNA clone of *lin-15a* was obtained from P. Sternberg (California Institute of Technology, Pasadena). Inserts into pPD129.36 were of the following sizes: *lin-35*, 2.7-kb cDNA spanning exons 3–10. *fzr-1*, 750-bp genomic spanning exons 1–2. *lin-23*, 1.1-kb genomic spanning exons 2–5. *lin-15a*, 1.1-kb cDNA spanning exons 2–6. *chd-4*, 1.4-kb genomic spanning exons 1–2. *efl-1*, 370-bp cDNA spanning exons 1–3. *lin-36*, 1.0-kb cDNA span-

ning exons 3–5. *hda-1*, 1.4-kb cDNA spanning exons 1–4. *lin-53*, 1.3-kb insert spanning exons 1–3.

fzr-1 subclones pDF63 contains a 7960-bp *Xba*I/*Sal*I fragment from cosmid ZK1307 subcloned into pBluescript. pDF65 contains a 3250-bp PCR-amplified fragment from the 5′ UTR of *fzr-1* cloned into plasmid pPD95.69 (gift of A. Fire). The construct creates an in-frame fusion of GFP containing an NLS to the first 6 amino acids of *fzr-1*.

Cyclin heat-shock constructs Full-length cyclin A cDNA from clone yk610 (from Y. Kohara) was amplified and inserted into pPD49.78 and pPD49.83 heat-shock vectors (from A. Fire). Cyclin E-heat shock vectors were a gift of M. Krause (NIH, Bethesda, MD).

Screen methodology

lin-35(n745); lin-8(n111) (MT1624) animals were injected with a mixture of cosmid C32F10 (100 µg/µL; Gu et al. 1998) and *sur-5::GFP* (100 µg/µL) to generate multiple independent strains carrying stable extrachromosomal arrays. Array *kuEx119* suppressed expression of the Muv phenotype in >90% of *lin-35; lin-8* double mutants and showed an ~75% transmission frequency. After crossing out the *lin-8* mutation to generate strain MH1461, animals were mutagenized with ethylmethanesulfonate (EMS) using standard procedures (Sulston and Hodgkin 1988). An F_2 clonal screen was carried out in which four F_2 animals were cloned per F_1 (for additional details, see Results), resulting in an expected coverage of ~1.35 haploid genomes per F_1 animal. Based on this estimate, we have screened ~3500 haploid genomes, or ~2500 F_1 (10,000 F_2) clones, to obtain seven unlinked mutations.

Mapping

Positional mapping of *fzr-1* presented a number of technical challenges: (1) both *fzr-1(ku298)* and *lin-35(n745)* single mutants lack discernable plate phenotypes; (2) double-mutant animals are nonviable and difficult to distinguish under a dissecting scope; and (3) the severity of the double-mutant phenotype can be at least partially suppressed by maternal products. These difficulties were circumvented by the procedures described below.

Two- and three-point mapping Triple-mutant mapping strains carrying *lin-35(n745)* and two linked visible marker mutations (e.g., *dpy* and *unc*) were generated for each chromosome. Homozygous *lin-35* males were mated to mapping strains, and male cross progeny were in turn mated to strain MH1621 (*fzr-1; lin-35; kuEx119*). *kuEx119*[+] cross progeny that segregated the marker mutations were then identified and used for either two- or three-point mapping.

For two-point mapping, ~100 *kuEx119*[+] wild-type sibling animals were cloned to single plates and, based on the segregated progeny, were scored as either homozygous or nonhomozygous for *ku298* and plus or minus for the marker mutations. *ku298* showed strong linkage to markers on LGII: 31/31 *ku298* homozygous animals failed to segregate *dpy-10*, *unc-4* markers, and 25/26 *ku298* homozygous animals failed to segregate *bli-2*, *rol-6* markers.

For three-point mapping, *kuEx119*[+] sibling recombinants (e.g., Dpy–non-Unc) were identified and allowed to self-fertilize. Then 10–15 *kuEx119*[+] self-progeny of the recombinant phenotype were cloned, allowed to self-fertilize, and then scored both for the presence of homozygous *ku298* and of the recombinant chromosomes.

We obtained the following data for three-point mapping of *ku298*: 3/19 *unc-4*–non-*dpy-10* recombinants acquired *ku298*; 28/29 *bli-2*–non-*rol-6* recombinants acquired *ku298*; 0/5 *rol-6*–non-*bli-2* recombinants acquired *ku298*; 9/38 *unc-4*–non-*let-23* recombinants acquired *ku298*.

SNP mapping We constructed the triple mutant strain MH1832 (*dpy-10*, *ku298*, *unc-4*) and verified the strain's ability to phenocopy the *lin-35; ku298* double-mutant phenotype using *lin-35(RNAi)* feeding methods (Fraser et al. 2000). MH1832 hermaphrodites were then mated to CB4856 homozygous males, and hermaphrodite cross progeny were cloned and allowed to self-fertilize. Recombinant animals (e.g., Unc–non-Dpy) were identified, and homozygous recombinant animals were isolated in the next generation and tested for the presence of *ku298* using *lin-35(RNAi)*. Predicted SNPs in the region were identified using the *C. elegans* SNP database and were further verified by experimentation.

We obtained the following mapping data for SNP vr77f08.s1@477 on cosmid T15H9: For Unc–non-Dpy recombinants that retained *ku298*, 54/54 were N2 for the SNP; 7/7 Unc–non-Dpy recombinants that lost *ku298* were CB4856 for the SNP; 5/5 Dpy–non-Unc recombinants that retained *ku298* were N2 for the SNP. For SNP vr89b04.s1@165 on cosmid T10B9 the following data were obtained: 2/7 Unc–non-Dpy recombinants that lost *ku298* were CB4856 for the SNP; 3/5 Dpy–non-Unc recombinants that retained *ku298* were CB4856 for the SNP.

Other methods

Cosmid rescue Rescue was obtained by coinjection of either ZK1307 or pDF63 with pRF4 into MH1621 using standard procedures (Mello and Fire 1995). Rescued animals were fertile, *kuEx119*⁻, and showed a Rol phenotype.

RNAi RNAi was carried out according to standard methods (Fire et al. 1998; Fraser et al. 2000). DAPI staining was according to Sulston and Hodgkin (1988).

Phylogenetic analysis Phylogenetic analysis was carried out with PAUP (Swafford 2000) using neighbor joining and maximum parsimony analysis with 500 bootstrap replicates. For each bootstrap, 10 heuristic searches of random addition sequence replicates were carried out.

Cyclin heat-shock strains Strains containing temperature-inducible cyclin E or cyclin A expression vectors were generated by injecting corresponding pPD49.78- and pPD49.83-derived constructs (50 μg/μL each) along with *sur-5::GFP* (100 μg/μL) into *unc-4*, *fzr-1* animals to obtain multiple stable extrachromosomal lines (cyclin A, *fdEx1* and *fdEx2*; cyclin E, *fdEx6* and *fdEx7*). Crossing to N2 generated *Ex*⁺ lines in the wild-type background.

References

Blelloch, R., Anna-Arriola, S.S., Gao, D., Li, Y., Hodgkin, J. and Kimble, J. 1999. The *gon-1* gene is required for gonadal morphogenesis in *Caenorhabditis elegans*. *Dev. Biol.* **216:** 382–393.

Boxem, M. and van den Heuvel, S. 2001. *lin-35* Rb and *cki-1* Cip/Kip cooperate in developmental regulation of G1 progression in *C. elegans*. *Development* **128:** 4349–4359.

Brehm, A., Miska, E.A., McCance, D.J., Reid, J.L., Bannister, A.J., and Kouzarides, T. 1998. Retinoblastoma protein recruits histone deacetylase to repress transcription. *Nature* **391:** 597–601.

Ceol, C.J. and Horvitz, H.R. 2001. dpl-1 DP and efl-1 E2F act with lin-35 Rb to antagonize Ras signaling in *C. elegans* vulval development. *Mol. Cell* **7:** 461–473.

Chen, Z. and Han, M. 2001. *C. elegans* Rb, NuRD and Ras regulate lin-39-mediated cell fusion during vulval fates specification. *Curr. Biol.* **11:** 1874–1879.

Clark, S.G., Lu, X., and Horvitz, H.R. 1994. The *Caenorhabditis elegans* locus lin-15, a negative regulator of a tyrosine kinase signaling pathway, encodes two different proteins. *Genetics* **137:** 987–997.

Clarke, A.R., Maandag, E.R., van Roon, M., van der Lugt, N.M., van der Valk, M., Hooper, M.L., Berns, A., and te Riele, H. 1992. Requirement for a functional Rb-1 gene in murine development. *Nature* **359:** 328–330.

Classon, M. and Dyson, N. 2001. p107 and p130: Versatile proteins with interesting pockets. *Exp. Cell Res.* **264:** 135–147.

Cohen-Fix, O., Peters, J.M., Kirschner, M.W., and Koshland, D. 1996. Anaphase initiation in *Saccharomyces cerevisiae* is controlled by the APC-dependent degradation of the anaphase inhibitor Pds1p. *Genes & Dev.* **10:** 3081–3093.

Culotti, J.G., Von Ehrenstein, G., Culotti, M.R., and Russell, R.L. 1981. A second class of acetylcholinesterase-deficient mutants of the nematode *Caenorhabditis elegans*. *Genetics* **97:** 281–305.

Davies, A.G., Spike, C.A., Shaw, J.E., and Herman, R.K. 1999. Functional overlap between the mec-8 gene and five sym genes in *Caenorhabditis elegans*. *Genetics* **153:** 117–134.

Dawson, I.A., Roth, S., and Artavanis-Tsakonas, S. 1995. The *Drosophila* cell cycle gene fizzy is required for normal degradation of cyclins A and B during mitosis and has homology to the CDC20 gene of *Saccharomyces cerevisiae*. *J. Cell Biol.* **129:** 725–737.

DeGregori, J., Kowalik, T., and Nevins, J.R. 1995. Cellular targets for activation by the E2F1 transcription factor include DNA synthesis- and G1/S-regulatory genes. *Mol. Cell. Biol.* **15:** 4215–4224.

de Nooij, J.C., Letendre, M.A., and Hariharan, I.K. 1996. A cyclin-dependent kinase inhibitor, Dacapo, is necessary for timely exit from the cell cycle during *Drosophila* embryogenesis. *Cell* **87:** 1237–1247.

Deshaies R.J. 1999. SCF and Cullin/Ring H2-based ubiquitin ligases. *Annu. Rev. Cell. Dev. Biol.* **115:** 435–467.

Dou, Q.P., Zhao, S., Levin, A.H., Wang, J., Helin, K., and Pardee,

A.B. 1994. G1/S-regulated E2F-containing protein complexes bind to the mouse thymidine kinase gene promoter. *J. Biol. Chem.* **269:** 1306–1313.

Du, W. and Dyson, N. 1999. The role of RBF in the introduction of G1 regulation during *Drosophila* embryogenesis. *EMBO J.* **18:** 916–925.

Dunaief, J.L., Strober, B.E., Guha, S., Khavari, P.A., Alin, K., Luban, J., Begemann, M., Crabtree, G.R., and Goff, S.P. 1994. The retinoblastoma protein and BRG1 form a complex and cooperate to induce cell cycle arrest. *Cell* **79:** 119–130.

Duronio, R.J. and O'Farrell, P.H. 1995. Developmental control of the G1 to S transition in *Drosophila*: Cyclin E is a limiting downstream target of E2F. *Genes & Dev.* **9:** 1456–1468.

Dyson, N. 1998. The regulation of E2F by pRB-family proteins. *Genes & Dev.* **12:** 2245–2262.

Fay, D.S. and Han, M. 2000. The synthetic multivulval genes of *C. elegans*: Functional redundancy, Ras-antagonism, and cell fate determination. *Genesis* **26:** 279–284.

Ferguson, E.L. and Horvitz, H.R. 1989. The multivulva phenotype of certain *Caenorhabditis elegans* mutants results from defects in two functionally redundant pathways. *Genetics* **123:** 109–121.

Ferguson, E.L., Sternberg, P.W., and Horvitz, H.R. 1987. A genetic pathway for the specification of the vulval cell lineages of *Caenorhabditis elegans*. *Nature* **326:** 259–267.

Fire, A., Xu, S., Montgomery, M.K., Kostas, S.A., Driver, S.E., and Mello, C.C. 1998. Potent and specific genetic interference by double-stranded RNA in *Caenorhabditis elegans*. *Nature* **391:** 806–811.

Flemington, E.K., Speck, S.H., and Kaelin, W.G., Jr. 1993. E2F-1-mediated transactivation is inhibited by complex formation with the retinoblastoma susceptibility gene product. *Proc. Natl. Acad. Sci.* **90:** 6914–6918.

Francis, R., Barton, M.K., Kimble, J., and Schedl, T. 1995. gld-1, a tumor suppressor gene required for oocyte development in *Caenorhabditis elegans*. *Genetics* **139:** 579–606.

Fraser, A.G., Kamath, R.S., Zipperlen, P., Martinez-Campos, M., Sohrmann, M., and Ahringer, J. 2000. Functional genomic analysis of *C. elegans* chromosome I by systematic RNA interference. *Nature* **408:** 325–330.

Fukushige, T., Hawkins, M.G., and McGhee, J.D. 1998. The GATA-factor elt-2 is essential for formation of the *Caenorhabditis elegans* intestine. *Dev. Biol.* **198:** 286–302.

Gu, T., Orita, S., and Han, M. 1998. *Caenorhabditis elegans* SUR-5, a novel but conserved protein, negatively regulates LET-60 Ras activity during vulval induction. *Mol. Cell. Biol.* **18:** 4556–4564.

Harbour, J.W. and Dean, D.C. 2000. The Rb/E2F pathway: Expanding roles and emerging paradigms. *Genes & Dev.* **14:** 2393–2409.

Hedgecock, E.M. and White, J.G. 1985. Polyploid tissues in the nematode *Caenorhabditis elegans*. *Dev. Biol.* **107:** 128–133.

Helin, K., Harlow, E., and Fattaey, A. 1993. Inhibition of E2F-1 transactivation by direct binding of the retinoblastoma protein. *Mol. Cell. Biol.* **13:** 6501–6508.

Hobert, O., D'Alberti, T., Liu, Y., and Ruvkun, G. 1998. Control of neural development and function in a thermoregulatory network by the LIM homeobox gene lin-11. *J. Neurosci.* **18:** 2084–2096.

Hodgkin, J. 2001. What does a worm need with 20,000 genes? *Genome Biol.* **2:** 2008.1–2008.4.

Hong, Y., Roy, R., and Ambros, V. 1998. Developmental regulation of a cyclin-dependent kinase inhibitor controls postembryonic cell cycle progression in *Caenorhabditis elegans*. *Development* **125:** 3585–3597.

Huang, L.S., Tzou, P., and Sternberg, P.W. 1994. The lin-15 locus encodes two negative regulators of *Caenorhabditis elegans* vulval development. *Mol. Biol. Cell* **5:** 395–411.

Irniger, S. and Nasmyth, K. 1997. The anaphase-promoting complex is required in G1 arrested yeast cells to inhibit B-type cyclin accumulation and to prevent uncontrolled entry into S-phase. *J. Cell Sci.* **110:** 1523–1531.

Irniger, S., Piatti, S., Michaelis, C., and Nasmyth, K. 1995. Genes involved in sister chromatid separation are needed for B-type cyclin proteolysis in budding yeast. *Cell* **81:** 269–278.

Jacks, T., Fazeli, A., Schmitt, E.M., Bronson, R.T., Goodell, M.A., and Weinberg, R.A. 1992. Effects of an Rb mutation in the mouse. *Nature* **359:** 295–300.

Johnson, C.D., Duckett, J.G., Culotti, J.G., Herman, R.K., Meneely, P.M., and Russell, R.L. 1981. An acetylcholinesterase-deficient mutant of the nematode *Caenorhabditis elegans*. *Genetics* **97:** 261–279.

Kaelin, W.G., Jr. 1999. Functions of the retinoblastoma protein. *Bioessays* **21:** 950–958.

King, R.W., Peters, J.M., Tugendreich, S., Rolfe, M., Hieter, P., and Kirschner, M.W. 1995. A 20S complex containing CDC27 and CDC16 catalyzes the mitosis-specific conjugation of ubiquitin to cyclin B. *Cell* **81:** 279–288.

Kipreos, E.T., Lander, L.E., Wing, J.P., He, W.W., and Hedgecock, E.M. 1996. cul-1 is required for cell cycle exit in *C. elegans* and identifies a novel gene family. *Cell* **85:** 829–839.

Kipreos, E.T., Gohel, S.P., and Hedgecock, E.M. 2000. The *C. elegans* F-box/WD-repeat protein LIN-23 functions to limit cell division during development. *Development* **127:** 5071–5082.

Krause, M. and Hirsh, D. 1987. A trans-spliced leader sequence on actin mRNA in *C. elegans*. *Cell* **49:** 753–761.

Lee, E.Y., Chang, C.Y., Hu, N., Wang, Y.C., Lai, C.C., Herrup, K., Lee, W.H., and Bradley, A. 1992. Mice deficient for Rb are nonviable and show defects in neurogenesis and haematopoiesis. *Nature* **359:** 288–294.

Lipinski, M.M. and Jacks, T. 1999. The retinoblastoma gene family in differentiation and development. *Oncogene* **18:** 7873–7882.

Lu, X. and Horvitz, H.R. 1998. lin-35 and lin-53, two genes that antagonize a *C. elegans* Ras pathway, encode proteins similar to Rb and its binding protein RbAp48. *Cell* **95:** 981–991.

Luo, R.X., Postigo, A.A., and Dean, D.C. 1998. Rb interacts with histone deacetylase to repress transcription. *Cell* **92:** 463–473.

Magnaghi-Jaulin, L., Groisman, R., Naguibneva, I., Robin, P., Lorain, S., Le Villain, J.P., Troalen, F., Trouche, D., and Harel-Bellan, A. 1998. Retinoblastoma protein represses transcription by recruiting a histone deacetylase. *Nature* **391:** 601–605.

McIntire, S.L., Reimer, R.J., Schuske, K., Edwards, R.H., and Jorgensen, E.M. 1997. Identification and characterization of the vesicular GABA transporter. *Nature* **389:** 870–876.

Mello, C. and Fire, A. 1995. DNA transformation. *Methods Cell Biol.* **48:** 451–482.

Morgan, D.O. 1999. Regulation of the APC and the exit from mitosis. *Nat. Cell Biol.* **1:** E47–E53.

Nevins, J.R. 2001. The Rb/E2F pathway and cancer. *Hum. Mol. Genet.* **10:** 699–703.

Nielsen, S.J., Schneider, R., Bauer, U.M., Bannister, A.J., Morrison, A., O'Carroll, D., Firestein, R., Cleary, M., Jenuwein, T., Herrera, R.E., et al. 2001. Rb targets histone H3 methylation and HP1 to promoters. *Nature* **412:** 561–565.

Nowak, M.A., Boerlijst, M.C., Cooke, J., and Smith, J.M. 1997. Evolution of genetic redundancy. *Nature* **388:** 167–171.

Ohtani, K., DeGregori, J., and Nevins, J.R. 1995. Regulation of the cyclin E gene by transcription factor E2F1. *Proc. Natl.*

Acad. Sci. **92:** 12146–12150.

Park, M., and Krause, M.W. 1999. Regulation of postembryonic G(1) cell cycle progression in *Caenorhabditis elegans* by a cyclin D/CDK-like complex. *Development* **126:** 4849–4860.

Schulze, A., Zerfass, K., Spitkovsky, D., Middendorp, S., Berges, J., Helin, K., Jansen-Durr, P., and Henglein, B. 1995. Cell cycle regulation of the cyclin A gene promoter is mediated by a variant E2F site. *Proc. Natl. Acad. Sci.* **92:** 11264–11268.

Schwab, M., Lutum, A.S., and Seufert, W. 1997. Yeast Hct1 is a regulator of Clb2 cyclin proteolysis. *Cell* **90:** 683–693.

Shi, Y. and Mello, C. 1998. A CBP/p300 homolog specifies multiple differentiation pathways in *Caenorhabditis elegans*. *Genes & Dev.* **12:** 943–955.

Sigrist, S.J. and Lehner, C.F. 1997. *Drosophila* fizzy-related down-regulates mitotic cyclins and is required for cell proliferation arrest and entry into endocycles. *Cell* **90:** 671–681.

Sigrist, S., Jacobs, H., Stratmann, R., and Lehner, C.F. 1995. Exit from mitosis is regulated by *Drosophila* fizzy and the sequential destruction of cyclins A, B and B3. *EMBO J.* **14:** 4827–4838.

Smith, V., Chou, K.N., Lashkari, D., Botstein, D., and Brown, P.O. 1996. Functional analysis of the genes of yeast chromosome V by genetic footprinting. *Science* **274:** 2069–2074.

Solari, F. and Ahringer, J. 2000. NURD-complex genes antagonise Ras-induced vulval development in *Caenorhabditis elegans*. *Curr. Biol.* **10:** 223–226.

Sprenger, F., Yakubovich, N., and O'Farrell, P.H. 1997. S-phase function of *Drosophila* cyclin A and its downregulation in G1 phase. *Curr. Biol.* **7:** 488–499.

Sudakin, V., Ganoth, D., Dahan, A., Heller, H., Hershko, J., Luca, F.C., Ruderman, J.V., and Hershko, A. 1995. The cyclosome, a large complex containing cyclin-selective ubiquitin ligase activity, targets cyclins for destruction at the end of mitosis. *Mol. Biol. Cell* **6:** 185–197.

Sulston, J.E. and Hodgkin, J. 1988. Methods. In *The nematode Caenorhabditis elegans* (eds. W.B. Wood and the Community of *C. elegans* Researchers), pp. 587–606. Cold Spring Harbor Laboratory Press, Cold Spring Harbor, NY.

Sulston, J.E. and Horvitz, H.R. 1977. Post-embryonic cell lineages of the nematode, *Caenorhabditis elegans*. *Dev. Biol.* **56:** 110–156.

Swafford, D.L. 2000. *PAUP phylogenetic analysis using parsimony (& other methods)*, version 4. Sinauer Associates, Sunderland, MA.

Tautz, D. 2000. A genetic uncertainty problem. *Trends Genet.* **16:** 475–477.

Terns, R.M., Kroll-Conner, P., Zhu, J., Chung, S., and Rothman, J.H. 1997. A deficiency screen for zygotic loci required for establishment and patterning of the epidermis in *Caenorhabditis elegans*. *Genetics* **146:** 185–206.

Thomas, J.H. and Horvitz, H.R. 1999. The *C. elegans gene* lin-36 acts cell autonomously in the lin-35 Rb pathway. *Development* **126:** 3449–3459.

Visintin, R., Prinz, S., and Amon, A. 1997. CDC20 and CDH1: A family of substrate-specific activators of APC-dependent proteolysis. *Science* **278:** 460–463.

von Zelewsky, T., Palladino, F., Brunschwig, K., Tobler, H., Hajnal, A., and Muller, F. 2000. The *C. elegans* Mi-2 chromatin-remodelling proteins function in vulval cell fate determination. *Development* **127:** 5277–5284.

Wagner, A. 2000. Robustness against mutations in genetic networks of yeast. *Nat. Genet.* **24:** 355–361.

Weintraub, S.J., Chow, K.N., Luo, R.X., Zhang, S.H., He, S., and Dean, D.C. 1995. Mechanism of active transcriptional repression by the retinoblastoma protein. *Nature* **375:** 812–815.

Winzeler, E.A., Shoemaker, D.D., Astromoff, A., Liang, H., Anderson, K., Andre, B., Bangham, R., Benito, R., Boeke, J.D., Bussey, H., et al. 1999. Functional characterization of the *S. cerevisiae* genome by gene deletion and parallel analysis. *Science* **285:** 901–906.

Zachariae, W. and Nasmyth, K. 1999. Whose end is destruction: Cell division and the anaphase-promoting complex. *Genes & Dev.* **13:** 2039–2058.

Zachariae, W., Schwab, M., Nasmyth, K., and Seufert, W. 1998. Control of cyclin ubiquitination by CDK-regulated binding of Hct1 to the anaphase promoting complex. *Science* **282:** 1721–1724.

Zhang, H.S., Gavin, M., Dahiya, A., Postigo, A.A., Ma, D., Luo, R.X., Harbour, J.W., and Dean, D.C. 2000. Exit from G1 and S phase of the cell cycle is regulated by repressor complexes containing HDAC-Rb-hSWI/SNF and Rb-hSWI/SNF. *Cell* **101:** 79–89.

Zheng, L. and Lee, W.H. 2001. The retinoblastoma gene: A prototypic and multifunctional tumor suppressor. *Exp. Cell Res.* **264:** 2–18.

Zur, A. and Brandeis, M. 2001. Securin degradation is mediated by fzy and fzr, and is required for complete chromatid separation but not for cytokinesis. *EMBO J.* **20:** 792–801.